Iron-Mediated N_2 Fixation

DOI: 10.1002/ange.201006299

Transformation of an $[Fe(\eta^2\text{-}N_2H_3)]^+$ Species to π-Delocalized $[Fe_2(\mu\text{-}N_2H_2)]^{2+/+}$ Complexes**

Caroline T. Saouma, R. Adam Kinney, Brian M. Hoffman, and Jonas C. Peters**

Several mechanisms have been proposed to describe the reduction of N_2 to NH_3 at the cofactor of MoFe nitrogenase.[1] Although experimental evidence is consistent with initial coordination of N_2 through a single metal center of the cofactor,[2] recent DFT studies have pointed to plausible diiron intermediates of the type $Fe_2(N_2H_y)$ ($y = 1$–4) en route to NH_3 formation.[3] In this context, it is noteworthy that diazene[4] and hydrazine[5] are readily reduced to NH_3 by nitrogenase under turnover conditions. Diiron model complexes that feature the $Fe_2(N_2H_y)$ core are therefore of timely interest,[6–8] especially as a spectral reference point to aid in the interpretation of ENDOR/ESEEM data that is being obtained with the enzymatic system during catalysis.[1d]

Herein we describe the characterization of an $[Fe(\eta^2\text{-}N_2H_3)]^+$ species that gives rise to a binuclear complex with an $[Fe_2(\mu\text{-}N_2H_2)]^{2+}$ core upon exposure to O_2. The latter complex is unique in that combined structural, spectroscopic, and DFT calculations suggest that the bridging "diazene" is best formulated as $N_2H_2^{2-}$. While this level of diazene activation has been observed in complexes of highly reducing early transition metals[9] it is not well established for the later transition metals, including iron.[7,10] One-electron reduction of the $[Fe_2(\mu\text{-}N_2H_2)]^{2+}$ complex furnishes the EPR-active mixed-valent $[Fe_2(\mu\text{-}N_2H_2)]^+$ complex, whose electronic structure characterization by combined EPR/ENDOR spectroscopy is described.

Entry to this chemical manifold arises from the addition of N_2H_4 to the iron alkyl precursor [(PhBP$_3$)FeMe] (**1**; PhBP$_3^-$ = PhB(CH$_2$PPh$_2$)$_3^-$) in the presence of a suitable trap. We have previously reported that the room temperature reaction between **1** and N_2H_4 quantitatively forms $[\{(PhBP_3)Fe\}_2(\mu\text{-}\eta^1\text{:}\eta^1\text{-}N_2H_4)(\mu\text{-}\eta^2\text{:}\eta^2\text{-}N_2H_2)]$, with concomitant loss of methane.[7b] A hydrazido complex of the type "$[(PhBP_3)Fe(N_2H_3)]$" is a plausible thermally unstable intermediate to invoke, and a strong-field trapping ligand was hence pursued. Addition of 1 equiv of N_2H_4 to **1** at −78 °C, followed by addition of 1 equiv of CO, affords orange $[(PhBP_3)Fe(\eta^2\text{-}N_2H_3)(CO)]$ (**2**) in ca. 70 % chemical yield (Scheme 1). Several side reactions compete with formation of **2**, and the crude reaction mixtures invariably contain $[\{(PhBP_3)Fe\}_2(\mu\text{-}\eta^1\text{:}\eta^1\text{-}N_2H_4)(\mu\text{-}\eta^2\text{:}\eta^2\text{-}N_2H_2)]$,[7b] $[(PhBP_3)Fe(CO)_2H]$ (see Supporting Information), and several other unidentified species. The similar solubilities of $[(PhBP_3)Fe(CO)_2H]$ and **2** diminish the isolated yield of **2** in analytically pure form.

The solid-state structure of **2** was obtained and indicates that the $N_2H_3^-$ ligand coordinates η^2 to the Fe center (Scheme 1). The Fe–N distances of 1.992(3) and 2.018(3) Å are as expected for coordination of sp^3-hybridized nitrogen to Fe, and are similar to those observed in the related six-

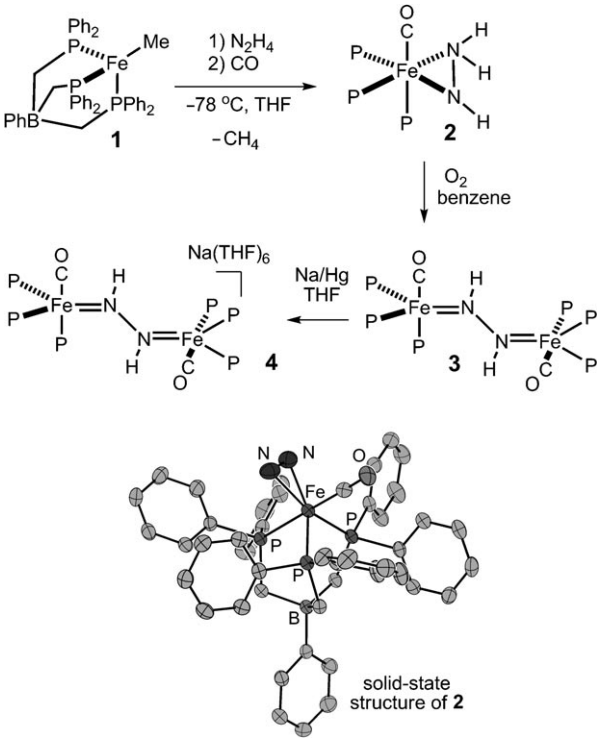

Scheme 1.

[*] C. T. Saouma,[+] Prof. J. C. Peters[+]
Department of Chemistry and Chemical Engineering
California Institute of Technology
1200 E. California Blvd, Pasadena, CA 91125 (USA)
E-mail: jpeters@caltech.edu
Homepage: http://jcpgroup.caltech.edu
R. A. Kinney, Prof. B. M. Hoffman
Department of Chemistry, Northwestern University
2145 Sheridan Road, Evanston, IL 60208 (USA)
E-mail: bmh@northwestern.edu
Homepage: http://chemgroups.northwestern.edu/hoffman/index.htm
[+] Former address: Department of Chemistry, Massachusetts Institute of Technology, Cambridge, MA 02139 (USA)

[**] We acknowledge the NIH (GM-070757, J.C.P.; HL 13531, B.M.H.) and the NSF (MCB0723330, B.M.H.). Funding for the Caltech NMR facility has been provided in part by the NIH (RR 027690) and funding for the MIT Department of Chemistry Instrumentation Facility has been provided in part by the NSF (CHE-0234877). The Betty and Gordon Moore Foundation supports the Molecular Observatory at Caltech. C.T.S. is grateful for an NSF graduate fellowship. Alec Durrell and Jens Kaiser provided guidance for resonance Raman and XRD experiments, respectively.

Supporting information for this article is available on the WWW under http://dx.doi.org/10.1002/anie.201006299.

coordinate [Fe(η^2-N_2H_4)] and [Fe(η^2-N_2H_2)] species.[8] The N1–N2 bond of 1.383(3) Å is shorter than expected for an N–N single bond, but consistent with that of a related $N_2H_3^-$ complex of tungsten.[11]

The ^{15}N NMR spectrum (−75 °C, [D$_8$]THF) of **2** shows a complicated signal centered around $\delta = 32$ ppm, which was fit to obtain chemical shifts and coupling constants (see Supporting Information). The NH–*N*H$_2$ and *N*H–NH$_2$ chemical shifts are noted at $\delta =$ 31.8 ppm and $\delta = 32.2$ ppm, respectively, with $^1J(N,N) = 10$ Hz. The ^{1}H NMR spectrum (−75 °C, [D$_8$]THF) of **2** shows three distinct protons for the hydrazido ligand that split into doublets when samples of **2** are prepared with $^{15}N_2H_4$. The N*H*–NH$_2$ chemical shift is noted at $\delta = 2.85$ ppm ($^1J(N,H) = 56$ Hz), and the inequivalent NH–N*H*$_2$ protons appear at $\delta = 6.55$ ppm ($^1J(N,H) = 86$ Hz) and $\delta =$ 1.88 ppm ($^1J(N,H) = 79$ Hz). The NMR data collectively indicates that the $N_2H_3^-$ ligand is comprised of two sp^3-hybridized nitrogen atoms.

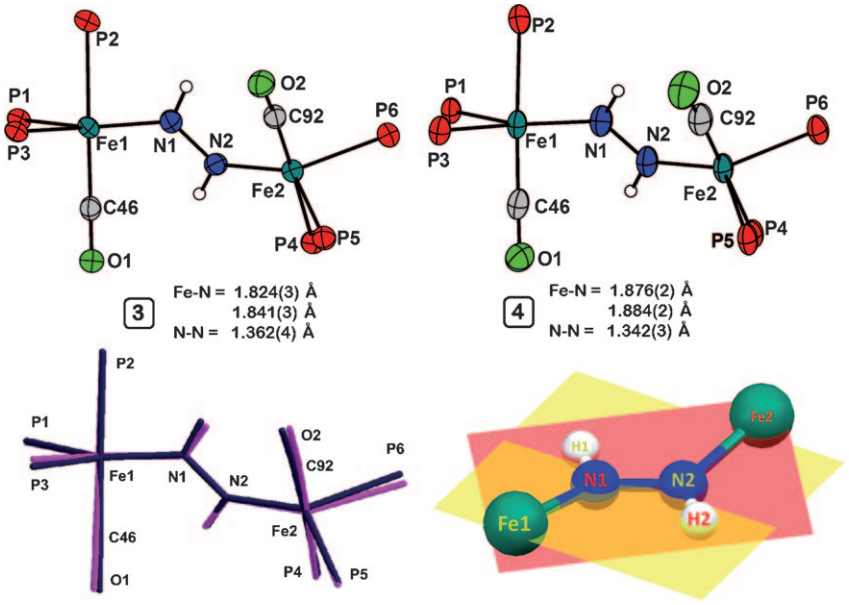

Figure 1. Displacement ellipsoid (50%) representations of the core atoms of **3** (left, top) and **4** (right, top), and an overlay of their core atoms (bottom, left; black, **3**; gray, **4**), and a representation showing the twist of the Fe-N-N-Fe linkage of **4** (bottom, right).

The orange hydrazido(−) complex **2** undergoes decay to the bridged blue diazene complex [{(PhBP$_3$)Fe(CO)}$_2$(μ-η^1:η^1-N_2H_2)] (**3**) in the presence of 0.5 equiv oxygen (Scheme 1). Other oxidants (e.g., Pb(OAc)$_4$, [Cp$_2$Fe$^+$], *p*-quinone), acids (e.g., pyridinium, FeCl$_3$, Sm(OTf)$_3$), and bases (e.g., N_2H_4, *n*BuLi, *t*BuN=P(cyclo-NC$_4$H$_8$)) were canvassed but do not facilitate this transformation. The reaction is solvent-dependent and proceeds in benzene but not in THF, perhaps owing to hydrogen bond stabilization of **2** by THF solvent (see Supporting Information).

The ^{15}N NMR spectrum of **3** (prepared from ^{15}N-**2**) displays a broad doublet at 292 ppm, indicative of an sp^2-hybridized nitrogen atom. The diazene protons are magnetically inequivalent, and the corresponding ^{1}H{^{31}P} NMR spectrum of **3** shows an AA′XX′ splitting pattern centered at $\delta = 9.5$ ppm. The chemical shifts of both the H and N atoms of the diazene ligand differ from those observed in the related [{(PhBP$_3$)Fe}$_2$(μ-η^1:η^1-N_2H_2)(μ-η^2:η^2-N_2H_2)] (^{15}N NMR: $\delta =$ 407.5, 58.0 ppm; ^{1}H NMR: $\delta = 13.20$, 4.16 ppm),[7b] and suggest that the extent of diazene activation in the two complexes may be different. Simulation of the ^{1}H{^{31}P} spectrum of **3** gives the following coupling constants: $^1J(N,H) = -71.0$ Hz, $^2J(N,H) = -2.1$ Hz, $^3J(H,H) = 14.8$ Hz, and $^1J(N,N) = 9.5$ Hz. The magnitude of the three-bond HH coupling is consistent with a *trans* configuration, and can furthermore be used as a probe for the extent of NN activation.[12] For example, $^3J(H,H) = 28.0$ Hz for [{(CO)$_5$Cr}$_2$(*trans*-μ-N_2H_2)],[13] which has an N–N bond distance of 1.25 Å,[14] while $^3J(H,H) =$ 9.4 Hz for [{(η^5-C$_5$Me$_4$H)$_2$ZrI}$_2$(*trans*-μ-N_2H_2)], which has an N–N bond distance of 1.414(3) Å.[9b] Hence, the observed ^3J(H,H) coupling in **3** is most consistent with a single bond.

The solid-state structure of **3** was obtained and its core atoms are shown in Figure 1 (see Supporting Information for complete structure). Both Fe centers have similar metrical parameters, and adopt a distorted trigonal bipyramidal geometry, with the approximate equatorial plane defined by two phosphorous and one nitrogen atom. The two Fe centers are related by a 133° rotation about the Fe–Fe vector. The *trans* protons on the diazene were located in the difference map, and form a planar diazene. However, the Fe-N-N-Fe linkage departs from planarity and features a 20.3° dihedral angle (Figure 1). The average Fe–N bond of 1.83 Å in **3** indicates the presence of π-bonding, while the elongated N–N bond of 1.362(4) Å establishes a significantly activated diazene unit. This distance is closer to that expected for an N(sp^2)–N(sp^2) single bond than that for a double bond (ca. 1.41 Å and 1.24 Å, respectively).[7,15]

Complex **3** is intensely colored and displays a transition at 716 nm ($\varepsilon = 8500\ M^{-1}\,cm^{-1}$) that is presumably charge transfer in nature by analogy to assignments made for similar bands observed for related dinuclear [M(η^1:η^1-N_2H_2)M] complexes.[10,16] The resonance Raman spectrum of **3** (633 nm excitation) contains an NN vibration at 1060 cm^{-1}, which shifts to 1032 cm^{-1} in samples of ^{15}N-enriched **3** (calculated shift for a diatomic harmonic oscillator: 1023 cm^{-1}). In addition, a second vibration is observed at 665 cm^{-1} (^{15}N: 651 cm^{-1}), which is tentatively assigned as the ν_s(FeN) vibration that couples with the NN vibration. Both of these vibrations are distinct from those measured by Lehnert et al. in an octahedral [Fe$_2$(μ-η^1:η^1-N_2H_2)] complex (ν(NN) = 1365 cm^{-1}; ν_{as}(FeN) = 496 cm^{-1}),[17] and consistent with appreciably stronger Fe–N and weaker N–N bonds in **3**. The combined structural, NMR, and vibrational data suggest that the diazene bridge in **3** might better be regarded as a dianionic hydrazido, $N_2H_2^{2-}$, as in the left resonance form shown in Figure 2B.

Cyclic voltammetry of **3** shows a reversible one-electron reduction event at −1.54 V (vs. Fc/Fc$^+$), and chemical treatment of **3** with 1 equiv of Na/Hg in THF cleanly generates the purple mixed-valence [Fe$_2$(μ-N_2H_2)]$^+$ complex, [{(PhBP$_3$)Fe}$_2$(μ-η^1:η^1-N_2H_2)][Na(THF)$_6$] (**4**). Crystals of **4**

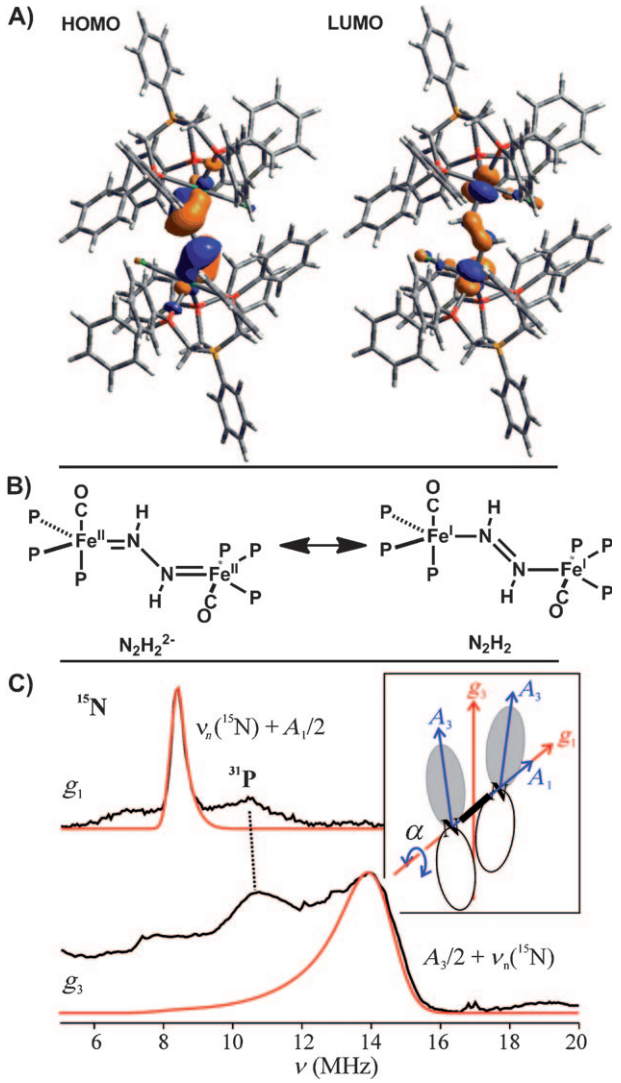

Figure 2. A) HOMO and LUMO of **3** (isocontour = 0.04); see the Supporting Information for computational details. B) Plausible resonance contributors to the electronic structure of **3**. C) 35 GHz Davies ^{15}N pulsed ENDOR spectra (black traces; ν_+ manifold ($\nu_+ = \nu_n + A/2$)) from ^{15}N-**4** at the indicated g values. Simulations (red, $\alpha = \pm 7°$; blue, $\alpha = 0°$ and 15°) use hyperfine and g tensors given in the text (see the Supporting Information); the ENDOR linewidth in the g_3 simulation is greater than that for g_1, as would be required by a distribution of α, see text.

suitable for XRD were grown by vapor diffusion of cyclopentane into a saturated THF solution of **4**.

The geometry of the $[Fe_2(\mu\text{-}N_2H_2)]^+$ core of **4** is very similar to that of the $[Fe_2(\mu\text{-}N_2H_2)]^{2+}$ core of **3**, as shown by an overlay of their core atoms (Figure 1). Upon reduction the average Fe–N distance increases by ca. 0.03 Å to 1.88 Å. Consistent with this, the ν_s(FeN) stretch decreases from 665 cm^{-1} to 643 cm^{-1} (^{15}N: 624 cm^{-1}) upon reduction.[18] The N–N bond distance in **4** is found to exhibit a marginal decrease to 1.342(3) Å upon reduction. These observations are collectively consistent with π-delocalization within the Fe-N-N-Fe core, with the unpaired electron populating an orbital that is predominantly Fe–N antibonding in character.

DFT calculations (see Supporting Information) were performed to further probe the electronic structures of both **3** and **4**. The frontier orbitals of **3** are isolobal to those of butadiene, and both the HOMO and LUMO are primarily composed of the Fe-N-N-Fe π-system. The HOMO displays Fe–N π-bonding and N–N π*-bonding character (Figure 2A). The LUMO features N–N π-bonding, and Fe–N π*-bonding character. Population of the LUMO should therefore result in a decrease in the N–N bond distance and an increase in the Fe–N bond distance. However, the SOMO of **4** has only minimal density on the N–N bridge, and so the actual change should be small, as observed. The observation that the reduction of **3** to **4** yields a shortened N–N distance in the N_2H_2 ligand in the present case is consistent with the DFT calculations. A similar result has been provided for a series of $[Mo_2(\mu\text{-}N_2)]^{6+/7+/8+}$ species where formal overall oxidation of the complex leads to a more "activated" bridging N_2 ligand.[19]

To further probe the electronic structure of the $[Fe_2(\mu\text{-}N_2H_2)]^+$ core of **4**, we turned to EPR/ENDOR spectroscopy. Complex **4** is paramagnetic, with a rhombic $S = {}^1/_2$ EPR signal (9:1 THF/MeTHF; $g = 2.125$, 2.040, 2.020) that remains essentially invariant from 77 K to 2 K. To test the model of a symmetrical, π-delocalized Fe-N-N-Fe core, 35 GHz ^{15}N electron-nuclear double resonance (ENDOR) measurements were performed at 2 K on ^{15}N-**4**.[20] Figure 2C displays ^{15}N ENDOR spectra selected from a 2D field–frequency pattern of ENDOR spectra (ν_+ manifold) collected across the EPR envelope of ^{15}N-**4** (see Supporting Information). The 2D pattern can be simulated with a single type of ^{15}N, having a nearly axial hyperfine coupling tensor, principal values, $\mathbf{A}(^{15}N) = +[6.7,\ 5.6,\ 17.8]$ MHz, isotropic coupling, a_{iso} (^{15}N) = 10 MHz, and anisotropic coupling, $\mathbf{T}(^{15}N) = +[-3.3, -4.5, 7.8]$ MHz (signs have been determined by pulsed ENDOR protocols; see Supporting Information).[21] The absence of a Mims ENDOR response associated with a second, more weakly coupled ^{15}N nucleus (not shown),[22] indicates that the two ^{15}N atoms from the bridge are magnetically equivalent and contribute equally to the ENDOR response depicted in Figure 2C, as expected for a delocalized $[Fe_2(\mu\text{-}N_2H_2)]^+$ ground state.

The strong anisotropy of **A** requires that the spin density on the two N atoms is of π character (A_3 parallel to the π orbital for each N).[23] The positive sign of **A** for ^{15}N indicates that the π spin density on the N–N bridge, $\rho^\pi(N)$, is negative (see Supporting Information), with the anisotropic coupling corresponding to $\rho^\pi(N) \approx -0.05$ spins per nitrogen. This small negative spin density on N arises from polarization of doubly occupied bonding core π orbitals by the large spin density on Fe. The DFT computations on **4** give $\rho^\pi(N) \approx -0.36$ spins per nitrogen, which is in satisfactory agreement with experiment given that DFT is well known to overestimate the effects of spin polarization.[24] This finding of rather low spin delocalization onto the bridging nitrogens of **4** illustrates why it is instructive to consider **3** in terms of the butadiene-like resonance structure shown in Figure 2B. The butadiene anion is the corresponding analogue to **4**, and its SOMO is minimally delocalized onto the central atoms. In **4**, delocalization would be decreased further due to the greater electronegativity of N compared to that of Fe.

The orientations of the ^{15}N hyperfine tensors also are informative. The observation of a single, very sharp ^{15}N

ENDOR feature at g_1 indicates the g_1 axis is coincident with the N–N vector and normal to the spin-bearing π orbitals on $^{15}N_i$ ($i = 1, 2$). These are expected to be primarily defined by the Fe_i-H_i-N_j ($j = 2, 1$) planes (Figure 1, bottom right), and thus lie essentially normal to the g_1 axis. Indeed, the 2D ENDOR pattern is satisfactorily simulated by taking the g_3 axis to bisect the angle between the two Fe_i-H_i-N_j planes, $2\alpha \approx 14°$, and then orienting each $^{15}N_i$ hyperfine tensor along the normal to its plane, which corresponds closely to simply rotating the hyperfine tensors of N1 and N2 around g_1 by equal and opposite angles, $\alpha \approx 7°$ (see Figure 2C, red trace).

The data does not define these rotations with precision; not only is agreement with experiment at g_2 improved with a $\alpha = 15°$ (see the Supporting Information), but also the observation of broad features in the ENDOR spectrum at g_3, in contrast to the narrow peak at g_1, suggest that there is a distribution of angles in the frozen solution, likely associated with torsions about the N–N "single" bond of as little as a few degrees. Overall, the ^{15}N ENDOR results support that **4**, at 2 K, contains a π-delocalized Fe-N-N-Fe core, as predicted by DFT computations, with the π-orbital "twist" indicated by the X-ray structure.

In summary, we have prepared an Fe(η^2-N_2H_3) species, and have shown that the coordinated hydrazido ligand is converted to diazene in the presence of oxygen. The end-on diazene ligands in the $[Fe_2(\mu\text{-}N_2H_2)]^{2+/+}$ cores of **3** and **4** are best regarded as "$N_2H_2^{2-}$", a bonding formulation previously observed for diazene complexes of highly reducing early transition metals. Combined structural, theoretical, and spectroscopic data for the dinuclear complex **3** indicate the presence of 4-center, 4-electron π-delocalized bonding across the Fe-N-N-Fe diiron μ-diazene core. This picture is consistent with DFT studies, as well as a combined EPR/ENDOR study of its one-electron reduced congener **4**. This electronic structure, in which the HOMO is N–N π-bonding, provides access to stable diazene complexes in both the $[Fe_2(\mu\text{-}N_2H_2)]^{2+/+}$ oxidation states. Whether such a fragment arises in the reaction pathway by which nitrogenase reduces N_2 to $2NH_3$ is being explored by detailed comparisons of the results presented here with ENDOR results for nitrogenase intermediates.[25]

CCDC 795818 (**2**), 795819 (**3**), 795820 (**4**), and 795821 ([$(PhBp_3)Fe(CO)_2H$]) contain the supplementary crystallographic data for this paper. These data can be obtained free of charge from The Cambridge Crystallographic Data Centre via www.ccdc.cam.ac.uk/data_request/cif.

Received: October 7, 2010
Revised: November 30, 2010
Published online: March 10, 2011

Keywords: diazene · ENDOR spectroscopy · hydrazido ligand · mixed-valence complexes · nitrogen fixation

[1] a) J. B. Howard, D. C. Rees, *Proc. Natl. Acad. Sci. USA* **2006**, *103*, 17088–17093; b) J. C. Peters, M. P. Mehn in *Activation of Small Molecules* (Ed.: W. B. Tolman), Wiley-VCH, Weinheim, **2006**, pp. 81–119; c) R. R. Schrock, *Angew. Chem.* **2008**, *120*, 5594–5605; *Angew. Chem. Int. Ed.* **2008**, *47*, 5512–5522; d) B. M. Hoffman, D. R. Dean, L. C. Seefeldt, *Acc. Chem. Res.* **2009**, *42*, 609–619.

[2] B. M. Barney, D. Lukoyanov, R. Y. Igarashi, M. Laryukhin, T. C. Yang, D. R. Dean, B. M. Hoffman, L. C. Seefeldt, *Biochemistry* **2009**, *48*, 9094–9102.

[3] a) B. Hinnemann, J. K. Nørskov, *J. Am. Chem. Soc.* **2004**, *126*, 3920–3927; b) J. Kästner, P. E. Blöchl, *J. Am. Chem. Soc.* **2007**, *129*, 2998–3006; c) I. Dance, *Dalton Trans.* **2010**, *39*, 2972–2983.

[4] B. M. Barney, J. McClead, D. Lukoyanov, M. Laryukhin, T. C. Yang, D. R. Dean, B. M. Hoffman, L. C. Seefeldt, *Biochemistry* **2007**, *46*, 6784–6794.

[5] B. M. Barney, T.-C. Yang, R. Y. Igarashi, P. C. Dos Santos, M. Laryukhin, H.-I. Lee, B. M. Hoffman, D. R. Dean, L. C. Seefeldt, *J. Am. Chem. Soc.* **2005**, *127*, 14960–14961.

[6] For [Fe(N_2H_3)] complexes see: a) J. L. Crossland, C. G. Balesdent, D. R. Tyler, *Dalton Trans.* **2009**, 4420–4422; b) Y. H. Lee, N. P. Mankad, J. C. Peters, *Nat. Chem.* **2010**, *2*, 558–565.

[7] For end-on diazene coordination see: a) D. Sellmann, J. Sutter, *Acc. Chem. Res.* **1997**, *30*, 460–469; b) C. T. Saouma, P. Müller, J. C. Peters, *J. Am. Chem. Soc.* **2009**, *131*, 10358–10359.

[8] For side-on diazene coordination see: a) L. D. Field, H. L. Li, S. J. Dalgarno, P. Turner, *Chem. Commun.* **2008**, 1680–1682; b) Ref. [7b].

[9] a) M. R. Churchill, Y. J. Li, L. Blum, R. R. Schrock, *Organometallics* **1984**, *3*, 109–113; b) W. H. Bernskoetter, J. A. Pool, E. Lobkovsky, P. J. Chirik, *J. Am. Chem. Soc.* **2005**, *127*, 7901–7911.

[10] K. Fujisawa, N. Lehnert, Y. Ishikawa, K.-i. Okamoto, *Angew. Chem.* **2004**, *116*, 5052–5055; *Angew. Chem. Int. Ed.* **2004**, *43*, 4944–4947.

[11] R. R. Schrock, A. H. Liu, M. B. O'Regan, W. C. Finch, J. F. Payack, *Inorg. Chem.* **1988**, *27*, 3574–3583.

[12] M. A. Cooper, S. L. Manatt, *J. Am. Chem. Soc.* **1969**, *91*, 6325–6333.

[13] M. R. Smith, T. Y. Cheng, G. L. Hillhouse, *J. Am. Chem. Soc.* **1993**, *115*, 8638–8642.

[14] G. Huttner, W. Gartzke, K. Allinger, *Angew. Chem.* **1974**, *86*, 860–861; *Angew. Chem. Int. Ed. Engl.* **1974**, *13*, 822–823.

[15] R. Allman in *The Chemistry of the Hydrazo, Azo, and Azoxy Groups* (Ed.: S. Patai), Wiley, New York, **1975**, p. 28.

[16] N. Lehnert, B. E. Wiesler, F. Tuczek, A. Hennige, D. Sellmann, *J. Am. Chem. Soc.* **1997**, *119*, 8869–8878.

[17] N. Lehnert, B. E. Wiesler, F. Tuczek, A. Hennige, D. Sellmann, *J. Am. Chem. Soc.* **1997**, *119*, 8879–8888.

[18] The presence of an additional CT band precluded our ability to obtain strong resonance enhancement, and the NN stretch could hence not be reliably located for **4**.

[19] J. J. Curley, T. R. Cook, S. Y. Reece, P. Müller, C. C. Cummins, *J. Am. Chem. Soc.* **2008**, *130*, 9394–9405.

[20] The ENDOR response for a ^{15}N nucleus ($I = 1/2$) in which $A > \nu_n$ is given by the equation $\nu = A/2 \pm \nu_n$. Mims and Davies 35 GHz pulsed ENDOR measurements: A. Schweiger, G. Jeschke, *Principles of Pulse Electron Paramagnetic Resonance*, Oxford University Press, Oxford, **2001**.

[21] a) T.-C. Yang, B. M. Hoffman, *J. Magn. Reson.* **2006**, *181*, 280–286; b) P. E. Doan, *J. Magn. Reson.* **2010**, DOI: 10.1016/j.jmr.2010.10.008.

[22] D. L. Tierney, H. Huang, P. Martásek, L. J. Roman, R. B. Silverman, B. M. Hoffman, *J. Am. Chem. Soc.* **2000**, *122*, 7869–7875.

[23] A. Carrington, A. D. McLachlan in *Introduction to Magnetic Resonance*, Harper & Row, New York, **1967**, p. 94.

[24] M. Radon', E. Broclawik, K. Pierloot, *J. Phys. Chem. B* **2010**, *114*, 1518–1528.

[25] Such comparisons are not straightforward because the Fe ions of nitrogenase presumed to bind substrate-derived species form part of the spin-coupled catalytic [Fe_7Mo] molybdenum–iron cofactor.

